Extracting transition rates from zero-polarizability spectroscopy

M. S. Safronova, Z. Zuhrianda, U. I. Safronova, and Charles W. Clark

Phys. Rev. A **92**, 040501 — Published 6 October 2015

DOI: 10.1103/PhysRevA.92.040501

How to extract transition rates from zero-polarizability spectroscopy

M. S. Safronova[1,2], Z. Zuhrianda[1], U. I. Safronova[3], and Charles W. Clark[2]

[1] *Department of Physics and Astronomy, University of Delaware, Newark, Delaware 19716*

[2] *Joint Quantum Institute, National Institute of Standards and Technology and the University of Maryland, Gaithersburg, Maryland, 20899-8410 and*

[3] *Physics Department, University of Nevada, Reno, Nevada 89557*

We predict a sequence of magic-zero wavelengths for the Sr excited $5s5p\,^3P_0$ state, and provide a general roadmap for extracting transition matrix elements using precise frequency measurements. We demonstrate that such measurements can serve as a best global benchmark of the spectroscopic accuracy that is required for the development of high-precision predictive methods. These magic-zero wavelengths are also needed for state-selective atom manipulation for implementation of quantum logic operations. We also identify five magic wavelengths of the $5s^2\,^1S_0 - 5s5p\,^3P_0$ Sr clock transition between 350 nm and 500 nm which can also serve as precision benchmarks.

PACS numbers: 37.10.Jk, 37.10.De, 32.10.Dk, 31.15.ac

The drive for increased precision in atomic, molecular, and optical (AMO) measurements has led to tighter tests of fundamental physics [1–3], transformational improvements in time and frequency metrology [4, 5], and suppression of decoherence in quantum information processing [6, 7]. Moreover, increases in AMO precision have resulted in the discovery of new applications such as: laboratory tests of time-variation of fundamental constants [8–10], searches for topological dark matter with atomic clocks [11] and magnetometers [12], probes of gravity and general relativity with atomic interferometry [13–15], and use of decoherence-free subspaces for Lorentz symmetry tests with entangled trapped ions [3].

For many of those applications, accurate knowledge of atomic properties has been critical for the design and interpretation of experiments, quantifying and reducing uncertainties and decoherence, and development of concepts for next-generation experiments and precision measurement techniques. Progress in development of high-precision theory [16–18] has yielded accurate predictions of many needed properties. In turn, high-precision measurements [19–24] have provided experimental benchmarks for refinement and improvement of theory.

Determination of transition matrix elements between excited states is a particulary difficult challenge for both theory and experiment. For example, the accuracy of theory has reached 0.2% for low-lying state transitions of alkali-metal atoms [16] and has attained 1% to a few percent accuracy for more complicated systems [25–27]. At present, further progress is hindered by scarcity of high-precision (better than 1%) benchmarks of transition amplitudes, which are important in many of the applications cited above. Heretofore, determination of transition matrix elements or transition rates between excited states have been based primarily upon the measurements of lifetimes and branching ratios, which seems very difficult to push beyond 1% accuracy. Very few such measurements are available, including the most recent $^3D_1$ lifetime measurement in Sr [4], where 0.5% uncertainty was achieved for the improved evaluation of the dynamic black-body shift. Moreover, such techniques face irreducible difficulties if the relevant branching ratios are small. This problem is particularly difficult for transitions involving excited states.

In this work, we provide a roadmap for extracting transition matrix elements using spectroscopic measurements of *frequency*. We make use of "magic-zero" frequencies at which the frequency-dependent polarizability, $\alpha(\omega)$, of a given atomic state vanishes [27, 28]. These magic-zero frequencies, which are analogues of interference phenomena encountered in classical coupled LC electrical circuits, are ubiquitous in accessible regions of the optical spectrum. We demonstrate that such frequency measurements can serve as a best global benchmark of high-precision atomic theory.

The magic-zero wavelengths were measured for the ground state of Rb [29, 30], K [31], and metastable He [32]. Thus, there is established experimental methodology to measure these quantities. The Rb measurement, which is based on finding the null point of diffraction of ultracold atoms by an optical lattice, was used to determine $5s - 6p$ matrix elements as was proposed in [33]. That determination attained an accuracy of 0.15-0.3% [29].

In this paper, we discuss a systematic approach to the determination of multiple transition probabilities using magic-zero spectroscopy and we describe its application to the important test case of the $5s5p\,^3P_0$ state of Sr. At present, this is one the best available benchmark systems for the following reasons:

- Well-developed experimental techniques are already established for Sr due to its prominence in atomic clock development [4] and studies of many-body effects in degenerate quantum gases [34, 35].
- The matrix element for the lowest-energy relevant

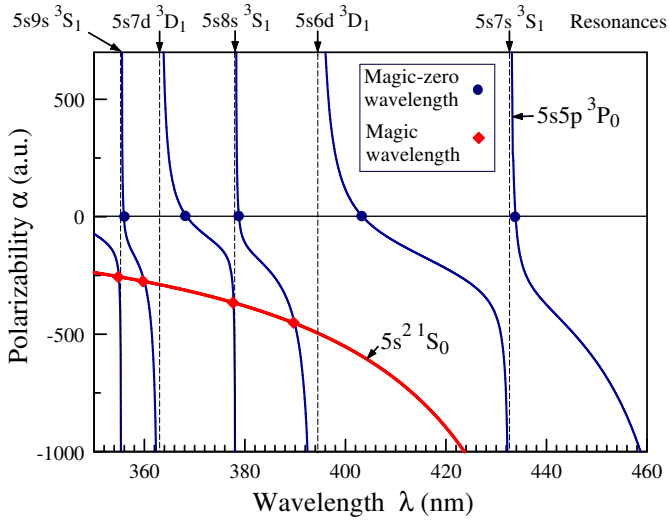

FIG. 1: (Color online) The dynamic polarizabilities of Sr $5s^2\ ^1S_0$ and $5s5p^3P_0$ states in the 350-460 nm wavelength range.

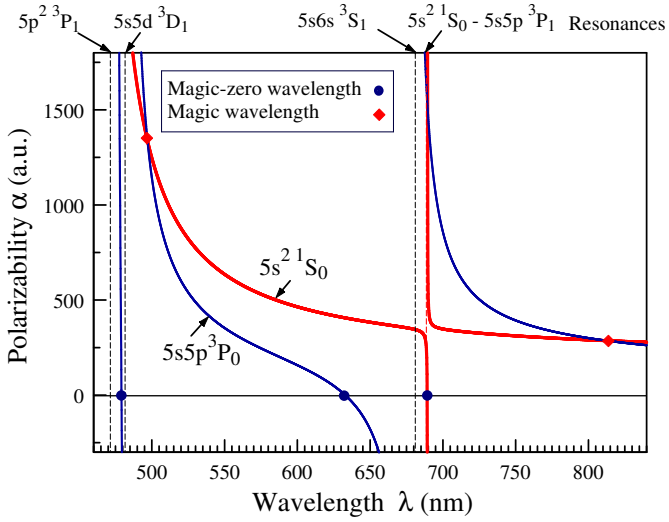

FIG. 2: (Color online) The dynamic polarizabilities of Sr $5s^2\ ^1S_0$ and $5s5p^3P_0$ states in the 460-840 nm wavelength range.

Sr transition, $5s5p^3P_0$-$5s4d\ ^3D_1$, is known with 0.23% accuracy from a recent $5s4d\ ^3D_1$ lifetime measurement [4]. This will simplify the extraction of matrix elements from $^3P_0$ to higher excited states.

- From a theoretical perspective, Sr is one of the best understood atoms with more than one valence electron, due to recent calculations of blackbody radiation (BBR) shift of the $5s^2\ ^1S_0$-$5s5p\ ^3P_0$ atomic clock transition [36].

In addition to precision measurement, there is another important application of the magic-zero wavelengths in the alkaline-earth atoms. The trapping potential in an optical lattice for a given atomic state is proportional to its dynamic polarizability $\alpha(\omega)$. For the magic-zero wavelength, $\alpha(\omega) = 0$, resulting in a vanishing ac Stark shift of that state. Thus, atoms in that state are insensitive to laser light of that frequency. This enables state-selective atom manipulation for the implementation of the quantum logic operations [37, 38]. In this work, we locate all of magic-zero wavelengths above 350 nm for both the ground and $^3P_0$ excited state of Sr.

Unless stated otherwise, we use the conventional system of atomic units, a.u., in which e, m_e, $4\pi\epsilon_0$ and the reduced Planck constant $\hbar$ have the numerical value 1. Polarizability in a.u. has the dimension of volume, and its numerical values presented here are expressed in units of a_0^3, where $a_0 \approx 0.052918$ nm is the Bohr radius. The atomic units for α can be converted to SI units via α/h [Hz/(V/m)^2]=$2.48832\times10^{-8}\alpha$ [a.u.], where the conversion coefficient is $4\pi\epsilon_0 a_0^3/h$ and the Planck constant h is factored out. Vacuum values are reported for all wavelengths.

We now demonstrate how to extract a set of matrix elements from a sequence of magic-zero wavelengths for Sr $5s5p\ ^3P_0$ state. Consider the standard expression for a frequency-dependent polarizability of a state v in terms of the sum over all other atomic states k [39]:

$$\alpha_0^v(\omega) = \frac{2}{3(2J+1)} \sum_k \frac{\langle k \|D\| v\rangle^2 (E_k - E_v)}{(E_k - E_v)^2 - \omega^2}. \qquad (1)$$

Here, J is the total angular moment of the state v and $\langle k \|D\| v\rangle$ are the reduced electric-dipole matrix elements which are the subject of the present work. In these equations, ω is assumed to be at least several line widths off resonance with the corresponding transitions. Linear polarization is assumed in all calculation.

It is self-evident from Eq. (1) that the contribution of state k to the sum changes sign as ω crosses the value $E_k - E_v$. *Magic-zero wavelengths* arise due to the cancellation of the contribution from a given resonant state k with the contributions from all of the other resonant states. Thus, there is a magic-zero wavelength between each pair of adjacent resonances, as can be seen in Figs.1 and 2. The actual location of each magic zero wavelength depends upon the distribution of electric-dipole matrix elements $\langle k \|D\| v\rangle$. Different matrix elements will be important for the determination of each magic zero-wavelength. Thus, measurement of a series of magic-zero wavelengths will enable one to extract the entire recommended set of the matrix elements for transitions to the $^3P_0$ state. Furthermore, we can obtain complementary information from *magic wavelengths* of the Sr $5s^2\ ^1S_0 - 5s5p\ ^3P_0$ clock transition, at which Stark shift of the clock transition vanishes. With such high-precision benchmarks established in one system to test a new theoretical approach, the theory can be applied to a large number of other systems where no experimental data are available.

TABLE I: Resonance wavelengths λ and reduced dipole matrix elements D in Sr. Vacuum wavelength values are given in nm. The recommended set of the matrix elements in a.u. is from [36]. [a]Ref. [4].

Transition	Wavelength		Matrix elements D	
	CI+all	Expt.	CI+all	Recomm.
$5s5p\ ^3P_0$ - $5s4d\ ^3D_1$	2642.4	2603.1	2.714	2.6707(62)[a]
$5s5p\ ^3P_0$ - $5s6s\ ^3S_1$	682.0	679.3	1.972	1.962(10)
$5s5p\ ^3P_0$ - $5s5d\ ^3D_1$	484.2	483.3	2.458	2.450(24)
$5s5p\ ^3P_0$ - $5p^2\ ^3P_1$	471.5	474.3	2.627	2.605(26)
$5s5p\ ^3P_0$ - $5s7s\ ^3S_1$	433.3	432.8	0.522	0.516(8)
$5s5p\ ^3P_0$ - $5s6d\ ^3D_1$	394.3	394.2	1.175	1.161(17)
$5s5p\ ^3P_0$ - $5s8s\ ^3S_1$	377.1	378.2	0.302	
$5s5p\ ^3P_0$ - $5s7d\ ^3D_1$	361.4	363.0	0.822	
$5s5p\ ^3P_0$ - $5s9s\ ^3S_1$	348.4	355.4	0.270	
$5s5p\ ^3P_0$ - $5s8d\ ^3D_1$	336.7	334.8	0.820	

TABLE II: Magic-zero $\lambda_{\rm zero}$ and magic $\lambda_{\rm magic}$ wavelengths. See text for the explanation of the recommended value calculations.

$\lambda_{\rm zero}$		$\lambda_{\rm magic}$	
CI+all-order	Recomm.	CI+all-order	Recomm.
$5s5p\ ^3P_0$		$5s^2\ ^1S_0 - 5s5p\ ^3P_0$	
	355.92		354.9
367.0	368.45	358.5	360.0
377.8	378.81	376.8	377.75
403.35	403.428	390.1	389.9
434.35	433.85		497.0
478.35	479.126		
634.7	632.83		
1672.9	1666.6		
$5s^2\ ^1S_0$			
679.55	689.20		

Sr has two valence electrons outside a closed Kr-like atomic core. The main challenge in the theoretical treatment of systems with two or more valence electrons is the accurate treatment of both core-valence correlations and strong valence-valence correlations. We use the hybrid approach introduced in [17] that combines configuration interaction (CI) and all-order linearized coupled-cluster methods. The core-valence (and core-core) correlations are treated by the coupled-cluster all-order method, which is used to construct the effective Hamiltonian. Then, this effective Hamiltonian is used in the configuration-interaction part of the method that treats the valence-valence correlations. Thus, all of the correlation correction to the wave functions is treated at the all-order level. Next, the resulting wave functions are used to evaluate matrix elements of various one-body operators, such as electric and magnetic mulitpole, magnetic and quadrupole hyperfine, and various P-odd and T-odd interactions. These matrix elements are also then used for evaluation of polarizabilities, P-odd and T-odd amplitudes, and long-range interaction coefficients C_6 and C_8. This approach is generally applicable for systems with several valence electrons and has a wide range of applications [25–27].

To determine the magic-zero wavelengths for the Sr $5s^2\ ^1S_0$ ground and $5s5p^3P_0$ excited states, we need to calculate their frequency dependent polarizabilities for a wide range of frequencies. The valence part of the polarizability is determined by solving the inhomogeneous equation of perturbation theory in the valence space, which is approximated as

$$(E_v - H_{\rm eff})|\Psi(v,M')\rangle = D_{{\rm eff},q}|\Psi_0(v,J,M)\rangle \qquad (2)$$

for a state v with the total angular momentum J and projection M [40]. While the $H_{\rm eff}$ includes the all-order corrections as described above, the effective dipole operator $D_{\rm eff}$ only includes random phase approximation (RPA) corrections at the present time.

A few other small corrections that include the core-Brueckner, two-particle, structural radiation, and normalization corrections can presently be calculated with second-order many-body theory [40–42]. Some of these corrections tend to contribute with an opposite sign leading to cancellations. These contributions were calculated for five electric-dipole matrix elements that give dominant contributions to the BBR shift of Sr lattice clock [36]. Total contributions of these four corrections ranged from 0.04% to 1.7%. As a result, these corrections to electric - dipole matrix elements contribute significantly in the $5s5p\ ^3P_0$ BBR shift calculation of Sr [36]. Their omission in earlier work [43] resulted in significant difference of the clock dc Stark shift with experiment [23]. The corrections are also very significant for the hyperfine constants [42].

The present bottleneck in the accuracy of this approach can be summarized as follows. The treatment of corrections to the matrix elements of the one-body electric-dipole operator $D_{\rm eff}$, and all of the other one-body operators mentioned above is limited to RPA and second-order many-body perturbation theory. We are currently developing a full all-order treatment of corrections to one-body operators, however there are essentially no experimental benchmarks that we can use to establish how well this approach will work. The measurements that we propose in this work will remedy this outstanding problem. We note that the method is non-specific for the particular type of the one-body operator and the advancement in the treatment of the dipole operator will also provide improvement for the other operators.

While we calculate the polarizabilities by solving the inhomogeneous equation (2), which accounts for the contribution from all bound and continuum states, we extract several dominant contributions from the low-lying bound states using the sum-over-states formula (1). To improve the accuracy of the calculations, we replace a few dominant terms in our polarizability calculations by their "recommended" values, which contain experimental energies and recommended matrix elements from Ref. [36], where available. To obtain recommended values for the $^3P_0$ state, the energies of the ten lowest transitions are

TABLE III: Breakdown by transition of the contributions (in a.u.) to dynamic polarizability of $5s5p\ ^3P_0$ state, at the eight magic-zero wavelengths indicated. The first ten rows give the contributions from the transitions indicated, and all other contribution are grouped together in row "Other". The chain of dominant contributions relevant to the extraction of matrix elements (see text for a discussion) is highlighted in bold.

Contribution	1666.6 nm	632.84 nm	479.127 nm	433.85 nm	403.429 nm	378.81 nm	368.45 nm	355.92 nm
$5s5p\ ^3P_0$ - $5s4d\ ^3D_1$	**-188.7**	-17.1	-9.5	-7.8	-6.7	-5.9	-5.6	-5.2
$5s5p\ ^3P_0$ - $5s6s\ ^3S_1$	**45.9**	**-251.4**	-37.9	-26.4	-20.8	-17.3	-15.9	-14.5
$5s5p\ ^3P_0$ - $5s5d\ ^3D_1$	**46.3**	**101.9**	**-2404**	-176.0	-97.5	-67.6	-58.9	-50.3
$5s5p\ ^3P_0$ - $5p^2\ ^3P_1$	**51.2**	**107.5**	**2361**	-241.2	-123.2	-82.9	-71.7	-60.7
$5s5p\ ^3P_0$ - $5s7s\ ^3S_1$	1.8	3.2	9.2	**337.9**	-11.2	-5.5	-4.4	-3.5
$5s5p\ ^3P_0$ - $5s6d\ ^3D_1$	8.2	12.7	24.1	44.6	**171.7**	-93.8	-53.8	-34.3
$5s5p\ ^3P_0$ - $5s8s\ ^3S_1$	0.5	0.8	1.3	2.1	4.2	**147.2**	-9.5	-3.9
$5s5p\ ^3P_0$ - $5s7d\ ^3D_1$	3.8	5.4	8.4	12.0	18.9	44.0	**122.7**	-89.1
$5s5p\ ^3P_0$ - $5s9s\ ^3S_1$	0.4	0.6	0.8	1.2	1.7	3.2	5.5	**142.7**
$5s5p\ ^3P_0$ - $5s8d\ ^3D_1$	3.4	4.6	6.4	8.1	10.6	15.1	18.9	28.6
Other	27.1	32.0	39.2	44.8	52.3	64.0	72.7	90.6
Total	0.0	0.0	-0.3	-0.7	0.0	0.4	0.0	0.4
Uncertainty in α	11.6	8.7	10.5	6.6	12	67	4.3	2.2
Uncertainty in λ_{zero}	0.1 nm	0.2 nm	0.05 nm	0.25 nm	0.05 nm	0.1 nm	0.6 nm	6 nm

replaced by the experimental values [44], five of the transition matrix elements are replaced by the recommended values from Ref. [36], and $5s5p\ ^3P_0 - 5s4d\ ^3D_1$ matrix elements is taken from [4]. For the $^1S_0$ state, the energies of the four lowest transitions and the $5s^2\ ^1S_0 - 5s5p\ ^1P_1$ matrix element is replaced by the experimental values [44, 45]. Both *ab initio* and recommended values are listed in Table I.

The dynamical polarizabilities of Sr $5s^2\ ^1S_0$ ground and $5s5p^3P_0$ excited states are plotted in Figs. 1 and 2. For clarity, we separate these into two wavelength region; 350-460 nm and 460-840 nm. All resonances from Table I are labeled on the top frame of the figures. For all of the $^3P_0$ resonances, we only write the upper transition states and omit $5s5p\ ^3P_0$ designations. The magic-zero wavelengths are determined by locating points where either $^3P_0$ or $^1S_0$ polarizabilities vanish. We also show magic wavelengths, where the $^3P_0$ and $^1S_0$ polarizabilities are identical. The 813.4 nm magic wavelength used for the Sr lattice clock [21] is shown near the right edge of Fig. 2. We note that our graphs show 5 other Sr magic wavelengths. The values of both magic-zero and magic wavelengths are summarized in Table II. Both *ab initio* and recommended values are listed. Our value of the $5s^2\ ^1S_0$ magic-zero wavelength agrees with the results of [37, 46]. Ref.[37] estimate of the $^3P_0$ magic-zero wavelength at 627 nm is 5 nm away from our 632.8(2) nm value.

The contributions from the 10 lowest resonant states to the $5s5p\ ^3P_0$ polarizabilities at the magic-zero wavelengths are given in the first 10 rows of Table III. The exact values of those wavelengths are given as the labels of the eight columns. "Other" contributions listed in Table III are obtained as the difference of the total polarizability value calculated by solving Eq. (2), and the sum of *ab initio* values for ten contributions explicitly listed in Table III. Therefore, "other" term includes all other transitions calculated in the *ab initio* CI+all-order+RPA approximation. This contribution smoothly varies with the wavelength and is substantially smaller than the dominant contributions for most magic-zero wavelengths. The sum of all contributions is zero within the numerical accuracy.

Table III demonstrates the use of the magic-zero wavelength measurements to establish experimental benchmarks for the transitions noted in bold font. First $5s5p\ ^3P_0 - 5s4d\ ^3D_1$ matrix element is already known from a precision lifetime measurement [4], so contributions in the first row are known with 0.5% precision. The matrix element of the second transition $5s5p\ ^3P_0 - 5s6s\ ^3S_1$ is constrained to 0.5% by the position of the 813.4 nm magic wavelength [36]; thus the values in the second row are known to about 1%.

We propose two methods for the extraction of the remaining matrix elements. First, a global fit of all measured magic-zero wavelength can be done, varying the dominant contributions to best match the experimental values of wavelength. Second, a simpler procedure can be used to extract the matrix elements sequentially by determination of dominant contributions, as follows

1. The dominant contributions of the third and fourth transitions in Table III, associated with the $5s5d\ ^3D_1$ and $5p^2\ ^3P_1$ states respectively, can be extracted from measurements of the first three magic-zero wavelengths. If all three are available, the uncertainty in the "Other" contribution can be established as well. The 479 nm wavelength is particulary useful, due to very large contributions of the third and fourth transitions. The correlation corrections are expected to be different for the transition to the $5p^2\ ^3P_1$ state in comparison to all other states, due to its different electron configuration (see Table II of Ref. [36]). Therefore, we recommend the precision measurement of 479 nm wavelength as a first priority.

2. With first four dominant contributions in hand, the fifth and sixth can be obtained independently from the 434 nm and 403 nm magic-zero wavelengths since only one of these transitions contributes significantly to its respective magic-zero wavelength. This happens because of the larger values of the $^3D_1$ matrix elements in comparison with those of $^3S_1$ for the higher states (see Table I).

3. Then, dominant contributions for the $5s8s\,^3S_1$, $5s7d\,^3D_1$, and $5s9s\,^3S_1$ transitions can be obtained if the last three wavelengths are known.

The magic wavelengths listed in Table II can be used as additional benchmarks in a similar way.

The uncertainties in the polarizability values and resulting estimated uncertainties in the magic-zero wavelengths are listed in the last two rows of Table III. The polarizability uncertainties are obtained by adding the estimated uncertainties in the each of ten contributions and uncertainties of the "Other" term in quadrature. The relative uncertainties in the polarizability contributions are twice the estimated relative uncertainties of the corresponding matrix elements listed in Table I. The uncertainties in the last four matrix elements were taken to be 3% and the uncertainty in the "Other" contribution was estimated at 5%.

In summary, we have predicted the values of nine magic-zero and five magic wavelengths for Sr. We demonstrated how measurements of these quantities may serve as a sensitive experimental benchmark for further development of higher-precision first-principles theory.

This research was performed under the sponsorship of the US Department of Commerce, National Institute of Standards and Technology, and was supported by the National Science Foundation under Physics Frontiers Center Grant PHY-0822671.

[1] W. C. Griffith, M. D. Swallows, T. H. Loftus, M. V. Romalis, B. R. Heckel, and E. N. Fortson, Phys. Rev. Lett. **102**, 101601 (2009).

[2] ACME Collaboration, J. Baron, W. C. Campbell, D. DeMille, J. M. Doyle, G. Gabrielse, Y. V. Gurevich, P. W. Hess, N. R. Hutzler, E. Kirilov, et al., Science **343**, 269 (2014).

[3] T. Pruttivarasin, M. Ramm, S. G. Porsev, I. I. Tupitsyn, M. S. Safronova, M. A. Hohensee, and H. Häffner, Nature (London) **517**, 592 (2015).

[4] T. Nicholson, S. Campbell, R. Hutson, G. Marti, B. Bloom, R. McNally, W. Zhang, M. Barrett, M. Safronova, G. Strouse, et al., Nature Comm. **6**, 6896 (2015).

[5] K. Beloy, N. Hinkley, N. B. Phillips, J. A. Sherman, M. Schioppo, J. Lehman, A. Feldman, L. M. Hanssen, C. W. Oates, and A. D. Ludlow, Phys. Rev. Lett. **113**, 260801 (2014).

[6] S. Zhang, F. Robicheaux, and M. Saffman, Phys. Rev. A **84**, 043408 (2011).

[7] E. A. Goldschmidt, D. G. Norris, S. B. Koller, R. Wyllie, R. C. Brown, J. V. Porto, U. I. Safronova, and M. S. Safronova, Phys. Rev. A **91**, 032518 (2015), 1503.02881.

[8] T. Rosenband et al., Science **319**, 1808 (2008).

[9] R. M. Godun et al., Phys. Rev. Lett. **113**, 210801 (2014).

[10] N. Huntemann, B. Lipphardt, C. Tamm, V. Gerginov, S. Weyers, and E. Peik, Phys. Rev. Lett. **113**, 210802 (2014).

[11] A. Derevianko and M. Pospelov, Nature Physics **10**, 933 (2014).

[12] S. Pustelny, D. Kimball, C. Pankow, M. P. Ledbetter, P. Wlodarczyk, P. Wcislo, M. Pospelov, J. R. Smith, J. Read, W. Gawlik, et al., Ann. Phys. **525**, 659 (2013).

[13] D. Schlippert, J. Hartwig, H. Albers, L. L. Richardson, C. Schubert, A. Roura, W. P. Schleich, W. Ertmer, and E. M. Rasel, Phys. Rev. Lett. **112**, 203002 (2014).

[14] G. Rosi, F. Sorrentino, L. Cacciapuoti, M. Prevedelli, and G. M. Tino, Nature (London) **510**, 518 (2014).

[15] M. G. Tarallo, T. Mazzoni, N. Poli, D. V. Sutyrin, X. Zhang, and G. M. Tino, Phys. Rev. Lett. **113**, 023005 (2014).

[16] S. G. Porsev, K. Beloy, and A. Derevianko, Phys. Rev. Lett. **102**, 181601 (2009).

[17] M. S. Safronova, M. G. Kozlov, W. R. Johnson, and Dansha Jiang, Phys. Rev. A **80**, 012516 (2009).

[18] S. G. Porsev, M. S. Safronova, and M. G. Kozlov, Phys. Rev. Lett. **108**, 173001 (2012).

[19] C. S. Wood, S. C. Bennett, D. Cho, B. P. Masterson, J. L. Roberts, C. E. Tanner, and C. E. Wieman, Science **275**, 1759 (1997).

[20] Z. W. Barber et al., Phys. Rev. Lett. **100**, 103002 (2008).

[21] A. D. Ludlow et al., Science **319**, 1805 (2008), 0801.4344.

[22] J. A. Keele, M. E. Hanni, S. L. Woods, S. R. Lundeen, and C. W. Fehrenbach, Phys. Rev. A **83**, 062501 (2011).

[23] T. Middelmann, S. Falke, C. Lisdat, and U. Sterr, Phys. Rev. Lett. **109**, 263004 (2012).

[24] K. Beloy, J. A. Sherman, N. D. Lemke, N. Hinkley, C. W. Oates, and A. D. Ludlow, Phys. Rev. A **86**, 051404 (2012).

[25] M. S. Safronova, V. A. Dzuba, V. V. Flambaum, U. I. Safronova, S. G. Porsev, and M. G. Kozlov, Phys. Rev. Lett. **113**, 030801 (2014).

[26] M. S. Safronova, S. G. Porsev, and C. W. Clark, Phys. Rev. Lett. **109**, 230802 (2012).

[27] M. S. Safronova, M. G. Kozlov, and C. W. Clark, Phys. Rev. Lett. **107**, 143006 (2011).

[28] L. J. Leblanc and J. H. Thywissen, Phys. Rev. A **75**, 053612 (2007).

[29] C. D. Herold, V. D. Vaidya, X. Li, S. L. Rolston, J. V. Porto, and M. S. Safronova, Phys. Rev. Lett. **109**, 243003 (2012).

[30] R. H. Leonard, A. J. Fallon, C. A. Sackett, and M. S. Safronova, arXiv:1507.07898.

[31] W. F. Holmgren, R. Trubko, I. Hromada, and A. D. Cronin, Phys. Rev. Lett. **109**, 243004 (2012).

[32] B. M. Henson, R. I. Khakimov, R. G. Dall, K. G. H. Baldwin, L.-Y. Tang, and A. G. Truscott, Phys. Rev. Lett. **115**, 043004 (2015).

[33] B. Arora, M. S. Safronova, and C. W. Clark, Phys. Rev. A **84**, 043401 (2011).
[34] X. Zhang, M. Bishof, S. L. Bromley, C. V. Kraus, M. S. Safronova, P. Zoller, A. M. Rey, and J. Ye, Science **345**, 1467 (2014).
[35] S. Stellmer, B. Pasquiou, R. Grimm, and F. Schreck, Phys. Rev. Lett. **110**, 263003 (2013).
[36] M. S. Safronova, S. G. Porsev, U. I. Safronova, M. G. Kozlov, and C. W. Clark, Phys. Rev. A **87**, 012509 (2013).
[37] A. J. Daley, M. M. Boyd, J. Ye, and P. Zoller, Phys. Rev. Lett. **101**, 170504 (2008).
[38] A. V. Gorshkov, A. M. Rey, A. J. Daley, M. M. Boyd, J. Ye, P. Zoller, and M. D. Lukin, Phys. Rev. Lett. **102**, 110503 (2009).
[39] J. Mitroy, M. S. Safronova, , and Charles W. Clark, J. Phys. B **43**, 202001 (2010).
[40] S. G. Porsev, Yu. G. Rakhlina, and M. G. Kozlov, Phys. Rev. A **60**, 2781 (1999).
[41] V. A. Dzuba, M. G. Kozlov, S. G. Porsev, and V. V. Flambaum, JETP **87**, 885 (1998).
[42] S. G. Porsev, Yu. G. Rakhlina, and M. G. Kozlov, J. Phys. B **32**, 1113 (1999).
[43] S. G. Porsev and A. Derevianko, Phys. Rev. A **74**, 020502 (2006).
[44] Kramida, A., Ralchenko, Yu., Reader, J., and NIST ASD Team (2012). NIST Atomic Spectra Database (ver. 5.0), [Online]. Available: http://physics.nist.gov/asd [2013, June 24]. National Institute of Standards and Technology, Gaithersburg, MD.
[45] M. Yasuda, T. Kishimoto, M. Takamoto, and H. Katori, Phys. Rev. A **73**, 011403 (2006).
[46] Y. Cheng, J. Jiang, and J. Mitroy, Phys. Rev. A **88**, 022511 (2013).